

PAPER • OPEN ACCESS

Effects of spatial resolution anisotropy on viscous terms using isotropic steady turbulence numerical analysis

To cite this article: Riku Hirabayashi *et al* 2021 *J. Phys.: Conf. Ser.* **2047** 012008

View the [article online](#) for updates and enhancements.

You may also like

- [Origin of magnetization-induced anisotropy of magnetic films](#)
Jin Han-Min, Chong-Oh Kim, Taek-Dong Lee et al.
- [Phase diagrams for anisotropic spin glasses](#)
A J Bray and L Viana
- [The magnetic anisotropy of Fe-SiO₂ and Fe₂₀Ni₈₀-SiO₂ granular solids](#)
Jian-Ping Wang, De-Hua Han, He-Lie Luo et al.



ECS
The
Electrochemical
Society
Advancing solid state &
electrochemical science & technology

DISCOVER
how sustainability
intersects with
electrochemistry & solid
state science research

Effects of spatial resolution anisotropy on viscous terms using isotropic steady turbulence numerical analysis

Riku Hirabayashi ¹, Hiroki Suzuki ^{2,*} and Shinsuke Mochizuki ¹

¹ Graduate School of Sciences and Technology for Innovation, Yamaguchi University, 2-16-1 Tokiwadai, Ube-shi, Yamaguchi 755-8611, Japan

² Graduate School of Natural Science and Technology, Okayama University, 3-1-1 Tsushima-naka, Kita-ku, Okayama-shi, Okayama 700-8530, Japan

E-mail: h.suzuki@okayama-u.ac.jp

Abstract. This study presents the effects of spatial resolution anisotropy on an isotropic turbulence field. Here, this turbulence field is steady. In order to set the anisotropy of the spatial resolution, the accuracy order of the viscosity terms is set to be anisotropic. The convection and viscosity terms are discretized using the second-order or fourth-order central difference schemes. The Reynolds number dependence of the turbulence statistics is used to examine this influence. The effects of resolution anisotropy on the small-scale turbulent field obtained by longitudinal derivatives as well as large-scale turbulent fields are small. On the other hand, the small-scale turbulent field obtained by lateral derivatives is significantly affected by the anisotropy of resolution in the low Reynolds number condition.

1. Introduction

Numerical analysis [1] is considered to be the third method in addition to experiments and theoretical analysis (e.g., [2,3]). The background to this is the rapid development and spread of computers in recent years. Numerical analysis is widely used industrially because it often has advantages in safety and low cost compared to experiments. Numerical analysis is a primary tool for fundamental research because it can simulate complex phenomena that are difficult to measure physically. In computational fluid dynamics, the governing equations of flows are solved numerically, and the flow field is reproduced by using computational resources to elucidate and predict various flow phenomena.

The central difference formula that discretizes the convection term appropriately without introducing high-order numerical viscosity is often used for simulating incompressible turbulence. Here, the high-order discretization schemes are also used for discretizing the convection terms. The accuracy for discretizing the viscous terms can also affect the observed results of the turbulence. The derivative terms discretized by using the finite-difference approximations are underestimated. Therefore, a sufficiently high spatial resolution should be set to be negligible the discretization error. Also, effects of conservation error of kinetic energy are often approached by previous works (e.g., [4]). This previous study proposed a series of discretization schemes for the convection terms with negligible conservation error of kinetic energy. This scheme is widely used to simulate incompressible flows by previous works.

There is previous works which focus on the effects of spatial resolution of viscous terms on steady turbulence (e.g., [5]). Spatial resolution can be anisotropic around the wall when turbulent flows on the wall are simulated. This study considers that the effects of small-scale anisotropy on the turbulence field should be studied. Therefore, the purpose of this study is to clarify the effects of small-scale anisotropy



due to the resolution anisotropy of viscous terms. To approach this issue, the present study focuses on the Reynolds number dependence of the turbulent kinetic energy and fundamental statistics in isotropic turbulence. We also investigate the Reynolds number dependency of statistics for quantitating the anisotropy of the small-scale turbulence.

Table 1. Numerical cases set based on the accuracy order for discretizing the convection and viscous terms.

Directions	Convection terms			Viscous terms		
	<i>x</i>	<i>y</i>	<i>z</i>	<i>x</i>	<i>y</i>	<i>z</i>
Case 222-222	2nd order	2nd order	2nd order	2nd order	2nd order	2nd order
Case 222-444	2nd order	2nd order	2nd order	4th order	4th order	4th order
Case 222-424	2nd order	2nd order	2nd order	4th order	2nd order	4th order
Case 444-444	4th order	4th order	4th order	4th order	4th order	4th order

2. Methods

The governing equations of the flow field are the continuity equation and the Navier-Stokes equations shown as follows:

$$\nabla \cdot \mathbf{u} = 0 \text{ and } \frac{\partial \mathbf{u}}{\partial t} + \mathbf{u} \cdot \nabla \mathbf{u} = -\nabla p + \frac{1}{\text{Re}} \nabla^2 \mathbf{u} + \mathbf{F}. \quad (1)$$

Here, \mathbf{u} , p and Re are velocity vector, pressure, and Reynolds number, respectively, and \mathbf{F} is an external force term according to the linear forcing method [6-8], and is given as follows.

$$\mathbf{F} = C\mathbf{u}^F. \quad (2)$$

This method is used to generate steady turbulence by giving a component of the external forcing term in proportion to the velocity component.

The components (u_x^F, u_y^F, u_z^F) of the velocity vector \mathbf{u}^F is given based on Goto and Vassilicos [9] as follows as the setting of the external force term that generates the isotropic steady turbulence.

$$\mathbf{u}_x^F = -\cos(x) \sin(y), \mathbf{u}_y^F = \sin(x) \cos(y), \text{ and } \mathbf{u}_z^F = \mathbf{0}. \quad (3)$$

These velocity components are set based on Taylor's analytical solution. Here, the velocity vector giving this external force term has the following characteristics:

$$\nabla \cdot \mathbf{u}^F = 0 \text{ and } \nabla^2 \mathbf{u}^F = -\mathbf{u}^F. \quad (4)$$

The external force term that produces the isotropic turbulence is set by combining the three components. The terms of external force applied are shown below.

$$\begin{aligned} u_x^F &= (2/\sqrt{3})(-\cos(x) \sin(y) + \cos(x) \sin(z)) \\ u_y^F &= (2/\sqrt{3})(-\cos(y) \sin(z) + \cos(y) \sin(x)) \\ u_z^F &= (2/\sqrt{3})(-\cos(z) \sin(x) + \cos(z) \sin(y)) \end{aligned} \quad (5)$$

The isotropic external force term also has the properties of Eq. (4), similar to the anisotropic external force term.

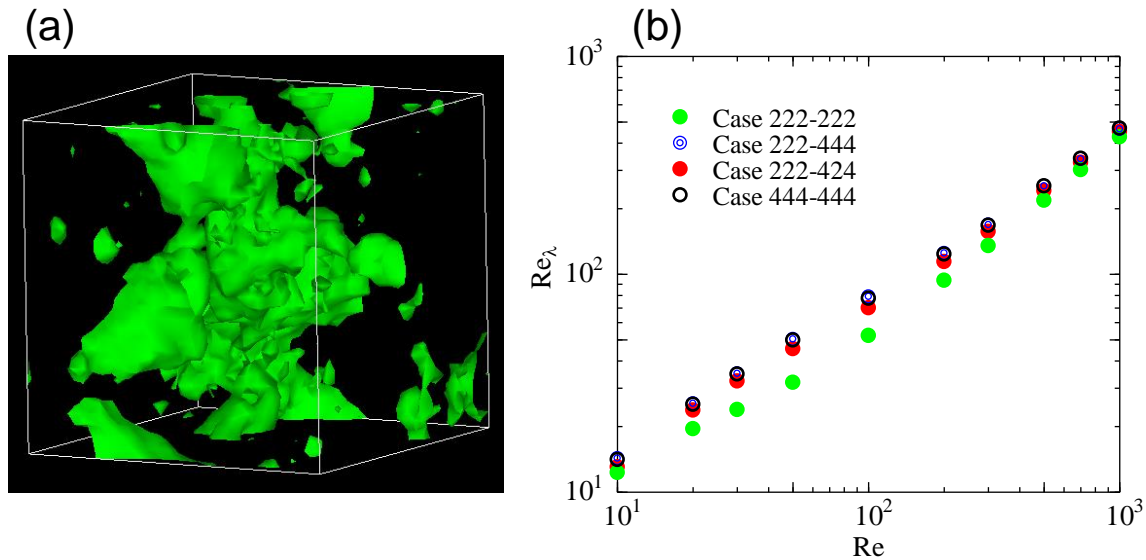


Figure 1. (a) Visualization of the instantaneous field of the present turbulence using isosurface of the static pressure fluctuation. (b) Turbulent Reynolds number as a function of computational Reynolds number Re .

The Smagolinsky model used in the LES is a vortex viscosity model with a typical length of filter width Δ and is the most basic SGS model that has been used for many years. The Smagolinsky model is based on the assumptions of local equilibrium and eddy viscosity [1]. The Smagolinsky model is equivalent to a zero equation model and there is no need to solve the transport equation when calculating the SGS stress. There is a parameter dependency that the optimum value of the model constant C_s differs depending on the flow field. In the present analysis, a value of C_s is set to 0.0573. This value of the model constant is given based on results of direct numerical simulation for isotropic turbulence.

The viscosity terms are linear and are analyzed by the second-order derivative. In the present analysis, the second-order and fourth-order difference schemes are used for discretizing the viscous terms. In the discretization of the viscosity term, the anisotropy of the spatial resolution is set by using the second-order scheme for the transverse direction and the fourth-order scheme for the two directions. The convection terms are discretized by second-order and fourth-order discretization schemes as used in a previous study [10]. Here skew-symmetric form is used for discretizing the convection terms. In the present analysis, kinetic energy conservation is explicitly held because of using the skew-symmetric form.

In this study, the numerical conditions were set as follows. The staggered grid system is used as the calculational grid. The size of the computational domain is $L^3 = (2\pi)^2$. The constant of the linear forcing is $C = 1$. The initial velocity field is isotropic flow field. The computational Reynolds number is $Re = 10, 20, 30, 50, 100, 200, 300, 500, 700, 1000$. The number of grid points is $N^3 = 32^3$. The time integration method is the fourth-order Runge-Kutta method. The pressure equation is solved using the fast Fourier transform. The fractional step method was applied to the coupling of the governing equations. Table 1 summarize present numerical cases.

3. Results and Discussion

Figure 1(a) shows the observed vortical structures for the condition of $Re = 300$ and pressure $p = -3$. Here the isosurface of static pressure fluctuation is used to visualize the large-scale structure. As shown in the figure, a typical large-scale structure is found in the present isotropic steady turbulence. Figure 1(b) shows the Reynolds number dependence of the turbulent Reynolds number. Here, the turbulent Reynolds number Re_λ is defined as follows:

$$\text{Re}_\lambda = \sqrt{\frac{\langle u^2 \rangle + \langle v^2 \rangle + \langle w^2 \rangle}{3}} \lambda \text{Re}, \text{ where } \lambda^2 = \left\{ \frac{\langle u^2 \rangle}{((du/dx)^2)} \frac{\langle v^2 \rangle}{((dv/dy)^2)} \frac{\langle w^2 \rangle}{((dw/dz)^2)} \right\}^{\frac{1}{3}}. \quad (6)$$

Where λ is the Taylor micro scale. As shown in the figure, the values of the turbulent Re number for Case 222-222 are smaller than those for the other cases. Because values for Case 222-444 agree with those for Case 444-444, the effects of the accuracy order for discretizing the convection terms are small. Values of the turbulent Reynolds number are larger than 150 for the computational Reynolds number values larger than 300. Therefore, small-scale turbulence is considered to be isotropic in the conditions of higher Reynolds numbers.

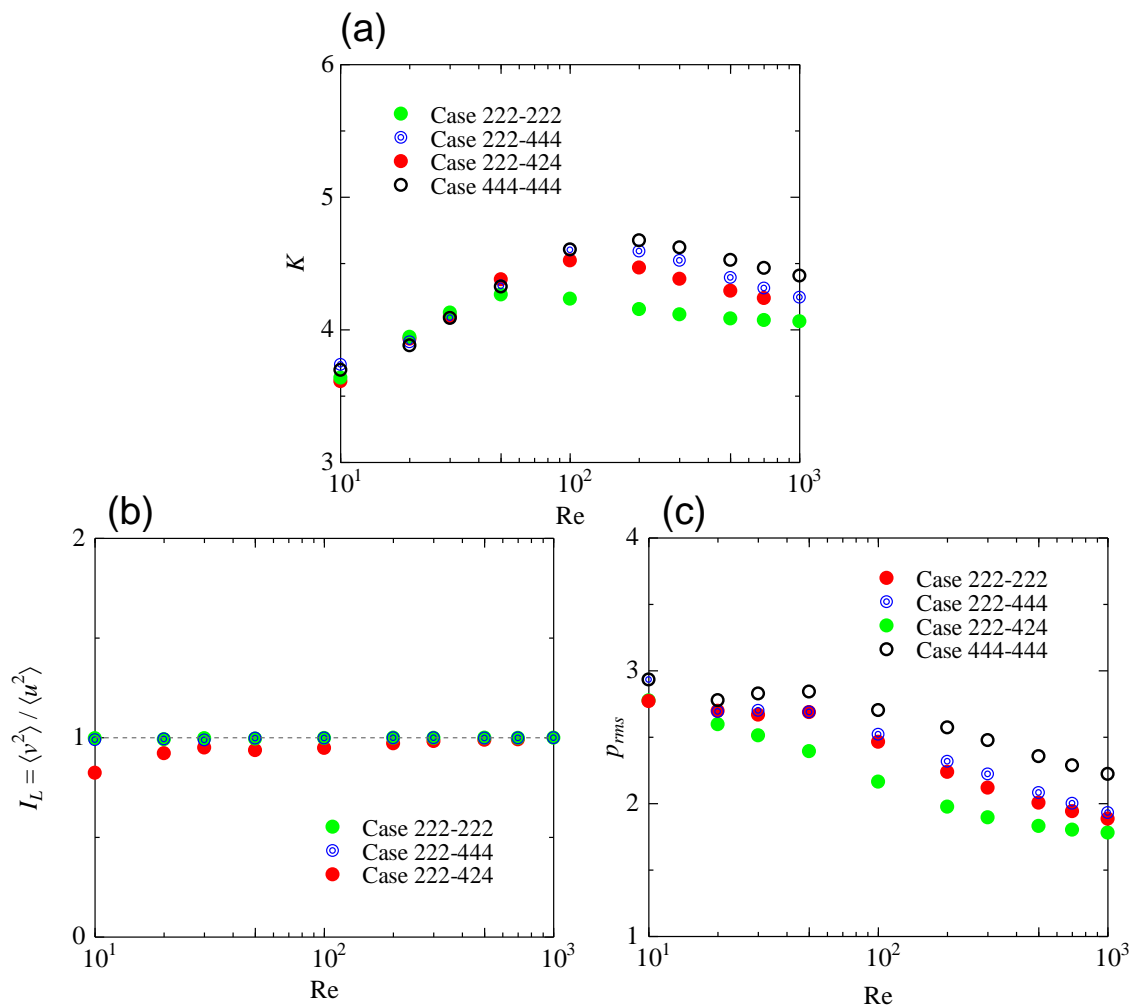


Figure 2. Turbulence statistics characterizing the large-scale structure. (a) Turbulent kinetic energy, (b) Large-scale anisotropy, and (c) root mean square value of statics pressure fluctuation.

Figure 2(a) shows the Reynolds number dependence of the turbulent kinetic energy. As shown in the results of Case 444-444, the profile of the turbulent kinetic energy has a local maximum around the condition of $\text{Re} = 200$. Values of Case 222-222 are found to be smaller than those of Case 444-444. By setting the higher-order accuracy for the viscous terms, this decrement can be reduced as compared to Case 222-444 with Case 222-222. As shown in the results, the difference in accuracy order of viscous

terms is significant in the results of the present analysis. Figure 2(b) shows the Reynolds number dependence of the large-scale anisotropy of velocity field. Here, the large-scale anisotropy is defined as follows: $I_L = \langle v^2 \rangle / \langle u^2 \rangle$. As shown in the figure, the anisotropy obtained for Case 222-222 and Case 222-444 is validated to be unity. Although, when the Reynolds number is small, there is a slight anisotropy in the results of Case 222-424, a value of the anisotropy approaches to unity for higher Reynolds number condition. Figure 2(c) shows the Reynolds number dependence of the root mean square (RMS) value of static pressure fluctuation (e.g., [11]). As shown in the results of Case 444-444, an RMS value is decreased as the computational Reynolds number increases in the higher Reynolds number region. Although results on the RMS values of static pressure fluctuation depend on the spatial resolution, the effects of the anisotropy of spatial resolution on the RMS values are small as comparing results of Case 222-444 to those of Case 222-424.

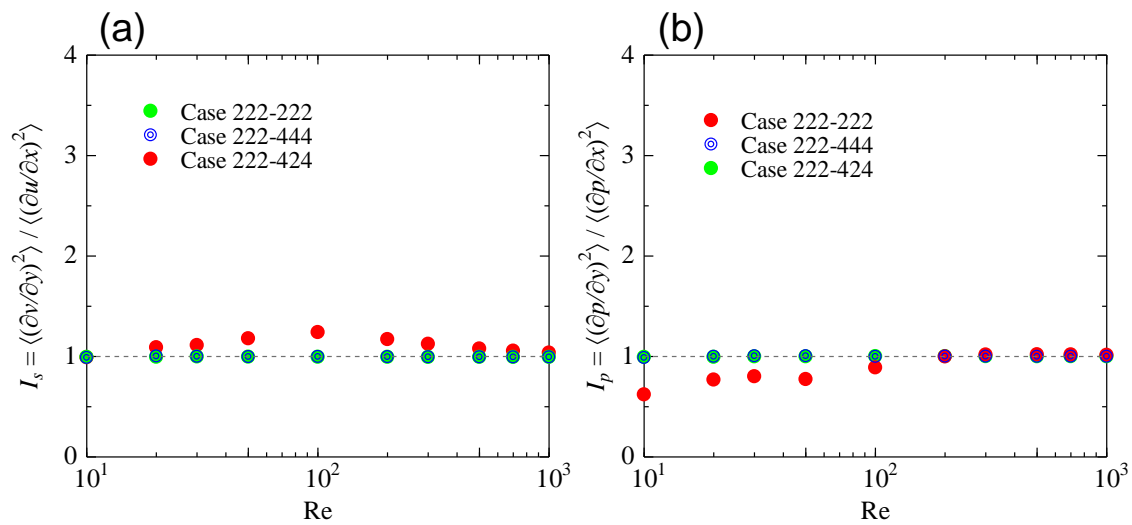


Figure 3. Effects of the spatial resolution anisotropy on the small-scale anisotropy. (a) small-scale anisotropy obtained using the longitudinal derivatives, and (b) small-scale anisotropy obtained using the static pressure fluctuation.

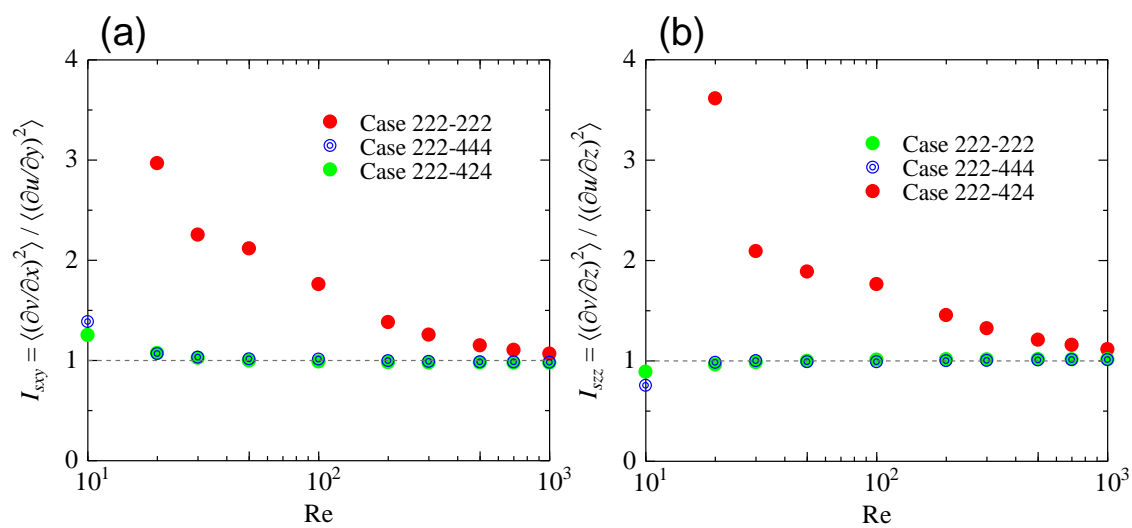


Figure 4. Effects of the spatial resolution anisotropy on the small-scale anisotropy obtained using the lateral derivatives. (a) I_{sxy} and (b) I_{szz} , where the definitions are shown in Equation (7).

Figure 3(a) shows the Reynolds number dependence on the small-scale anisotropy of the velocity field. Here, the anisotropy of the small-scale velocity field is defined as follows: $I_s = \langle (\partial v / \partial y)^2 \rangle / \langle (\partial u / \partial x)^2 \rangle$. As shown in the figure, the small-scale velocity field is isotropic for the results of Case 222-222 and Case 222-444. When the spatial resolution is anisotropic shown as in Case 222-424, there is the Reynolds number range where the small-scale velocity field is slightly anisotropic. Figure 3(b) shows the Reynolds number dependence on the small-scale anisotropy of the static pressure field. Here this anisotropy value is given as follows: $I_s = \langle (\partial p / \partial y)^2 \rangle / \langle (\partial p / \partial x)^2 \rangle$. As shown in the figure, in Case 222-222 and Case 222-444, where the spatial resolution is isotropic, the static pressure fluctuation field on a small scale is isotropic. The small-scale static pressure fluctuation field in Case 222-424 is slightly anisotropic. This anisotropy increases as the computational Reynolds number decreases.

In this study, in addition to the small-scale fluctuation field obtained using the longitudinal derivative, the anisotropy of the field obtained using the lateral derivative is also investigated. Here, two definitions are used in this study to calculate the anisotropy of the small-scale fluctuation field using the lateral derivative.

$$I_{sxy} = \frac{\langle (dv/dx)^2 \rangle}{\langle (du/dy)^2 \rangle} \text{ and } I_{szz} = \frac{\langle (dv/dz)^2 \rangle}{\langle (du/dz)^2 \rangle}. \quad (7)$$

As shown in Figure 4 (a) and (b), the fluctuation fields obtained in Case 222-222 and Case 222-444 are considered to be isotropic. On the other hand, the fluctuation field of Case 222-424 is significantly anisotropic. The magnitude of this anisotropy increases as the computational Reynolds number decreases. When the computational Reynolds number is small, the anisotropy obtained by using the lateral derivative of the fluctuation field of Case 222-424 is much larger than that obtained by using the longitudinal derivative.

4. Conclusions

The purpose of this study is to numerically study the fundamental characteristics of the generated steady turbulence by giving an isotropic external force term using the linear forcing method. In conducting the present analysis, we focused on the Reynolds number dependence of the turbulent statistics and the effect of the spatial resolution anisotropy of the viscous terms in the governing equations.

As shown in the results on the turbulent Reynolds number and the visualization results, the turbulent field used in this study is validated to be a turbulent flow sufficiently developed. Also, as shown in the results of the Reynolds number dependence of the large-scale turbulence statistics, spatial resolution accuracy of the viscous terms affects the turbulence statistics in the higher Reynolds number range.

For the results on the anisotropy of small-scale turbulence field, the effects of the spatial resolution anisotropy on the small-scale field are more significant in the anisotropy obtained using the lateral derivatives.

This study investigated the effects of spatial resolution anisotropy on the isotropic turbulent fields. In engineering applications, there are cases where anisotropic turbulence field, such as wall turbulence, is analyzed with anisotropic resolution. As a future study, the present study considers that the effects of anisotropic spatial resolution on the anisotropic turbulent field should be investigated.

Acknowledgments

This work was supported in part by the Japanese Ministry of Education, Culture, Sports, Science and Technology through Grants-in-Aid (Nos. 20H02069 and 21K03859). This work was supported (in part) by Grant for Environmental Research Projects from The Sumitomo Foundation.

References

- [1] Pope S B 2000 *Turbulent Flows*. Cambridge University Press
- [2] Suzuki H, Nagata K, Sakai Y, Hasegawa Y 2013 *Phys. Scr.* **2013** (T155) 014062
- [3] Suzuki H, Mochizuki S, Hasegawa Y 2018 *Flow Meas. Instrum.* **62** 1-8

- [4] Morinishi Y, Lund T S, Vasilyev O V, Moin P 1998 *J. Comput. Phys.* **143** 90-124
- [5] Suzuki H, Nagata K, Sakai Y, Hayase T, Hasegawa Y, Ushijima T 2013 *Int. J. Numer. Meth. Fluids* **73** 509-22
- [6] Lundgren T S 2003 *Ann Res. Briefs of Center for Turb. Res.* 461-73
- [7] Rosales C and Meneveau C 2005 *Phys. Fluids* **17** 095106
- [8] Carroll P L, Blanquart G 2013 *Phys. Fluids* **25** 105114
- [9] Goto S, Vassilicos J C 2015 *Phys. Lett. A* **379** 1144-8
- [10] Suzuki H, Nagata K, Sakai, Y, Hayase, T, Hasegawa, Y, Ushijima, T 2013 *Fluid Dyn. Res.* **45** 061409
- [11] Pumir A 1994 *Phys. Fluids* **6** 2071-83